Correspondence Relations Between Deflection, Buckling Load, and Frequencies of Thin Functionally Graded Material Plates and Those of Corresponding Homogeneous Plates

Shi-Rong Li
Department of Civil Engineering,
Yangzhou University,
Yangzhou, Jiangsu 225127, China;
Department of Biomedical
Engineering and Mechanics,
Virginia Polytechnic Institute and
State University,
Blacksburg, VA 24061

Xuan Wang
School of Hydraulic,
Energy and Power Engineering,
Yangzhou University,
Yangzhou, Jiangsu 225127, China

Romesh C. Batra
Fellow ASME
Department of Biomedical
Engineering and Mechanics,
Virginia Polytechnic Institute and
State University,
Blacksburg, VA 24061

Based on the classical plate theory (CPT), we derive scaling factors between solutions of bending, buckling and free vibration of isotropic functionally graded material (FGM) thin plates and those of the corresponding isotropic homogeneous plates. The effective material properties of the FGM plate are assumed to vary piecewise continuously in the thickness direction except for the Poisson ratio that is taken to be constant. The correspondence relations hold for plates of arbitrary geometry provided that the governing equations and boundary conditions are linear. When the stretching and bending stiffnesses of the FGM plate satisfy a relation, Poisson's ratio is constant and the boundary conditions are such that the in-plane membrane forces vanish, then there exists a physical neutral surface for the FGM plate that is usually different from the plate midsurface. Example problems studied verify the accuracy of scaling factors.

[DOI: 10.1115/1.4031186]

Keywords: nonhomogeneous plate, bending, buckling, free vibration, classical plate theory, correspondence relations

1 Introduction

Transversely nonhomogeneous plates with material properties varying through the thickness such as sandwich, laminated, and FGM plates are widely used in engineering structures. An FGM plate can be designed to have a desired variation of material properties in one or more directions. A widely used design has material properties varying only in the thickness direction. We note that Qian and Batra [1] and Liu et al. [2] have analyzed vibrations of a plate with material properties continuously varying in two directions. Whereas, Qian and Batra used a higher-order shear and normal deformation plate theory (HSNDT) and numerically solved the governing equations, Liu et al. provided a Levy-type solution for a rectangular plate with two opposite sides simply supported.

Jha et al. [3] and Swaminathan et al. [4] have reviewed works on bending, buckling and vibration of the FGM plates that have employed the CPT, the first-order shear deformation plate theory (FSDT), the higher-order shear deformation plate theory (HSDT), the HSNDT, and the three-dimensional linear elasticity theory. We note that in most engineering applications, the CPT is used to predict the structural behavior of thin plates. In view of the immense literature on the FGM plates, it is nearly impossible to review all the works here. Thus we limit ourselves to reviewing some of the works on the bending, buckling and free vibration of the FGM plates based on the CPT that are closely related to our work.

Yang and Shen [5] investigated free and forced vibration of in-plane stressed thin rectangular FGM plates resting on a two-parameter elastic foundation by the differential quadrature method (DQM). He et al. [6] studied the shape and vibration control of rectangular FGM plates with integrated piezoelectric sensors and actuators by using the finite element method (FEM) and the CPT. Javaheri and Eslami [7] analyzed buckling of simply supported rectangular FGM plates under different in-plane compressive loads and derived closed form solution for the critical buckling load. Samsarn Shariata et al. [8] extended the analytical method of Refs. [5,7] to investigate the critical buckling of simply supported rectangular FGM plates with geometric imperfections and subjected to in-plane compressive loads. Mohammadi et al. [9] derived a Levy type analytical solution for critical buckling of the rectangular FGM plates with two opposite edges simply supported and presented numerical results of the critical buckling load for different boundary conditions. Chi and Chung [10,11] studied static bending of simply supported rectangular FGM plates subjected to transverse distributed loads. Analytical solutions using Fourier series were obtained for Young's modulus varying in the thickness direction according to power-law, sigmoid, and exponential functions. Through numerical experiments, they showed that the effect of the variation in Poisson's ratio on the mechanical behavior of the FGM plates is very small. Whereas Poisson's ratio may not affect global quantities such as frequencies and buckling loads, it influences displacements as shown by Nie and Batra [12] and Zimmerman and Lutz [13].

By using B-splines to discretize the governing differential equation in the space domain, Yin et al. [14] numerically studied the free vibration response of thin rectangular FGM plates by introducing a physical neutral surface. Analytical investigation of the

Contributed by the Applied Mechanics Division of ASME for publication in the Journal of Applied Mechanics. Manuscript received April 21, 2015; final manuscript received July 27, 2015; published online August 21, 2015. Assoc. Editor: Glaucio H. Paulino.

free vibration response of thin circular and annular FGM plates integrated with two uniformly distributed actuator layers made of piezoelectric materials were carried out by Ebrahimi and Rastgo [15,16]. Mirtalaie and Hajabasi [17] analyzed free vibration of FGM thin annular sector plates by using the DQM. Hasani Baferani et al. [18] presented both the Navier and the Levy type solutions for free vibration of thin rectangular FGM plates under various boundary conditions. Vel and Batra [19–21] have provided exact solutions of static deformations, vibrations, and transient thermal stresses induced in the FGM plates using the three-dimensional linear elasticity theory.

Some authors have investigated nonlinear deformations of the thin FGM plates using the CPT and incorporating von Kármán's nonlinear strain–displacement relations. By using a semi-analytical approach, Yang and Shen [22] studied large deflection and postbuckling response of rectangular FGM plates resting on a two-parameter elastic foundation under transverse and in-plane loads. The nonlinear partial differential equations were solved by a perturbation technique. Nonlinear free vibration behavior of rectangular FGM plates was studied by Woo et al. [23] who used the Fourier series and presented numerical values of the fundamental frequency versus the centroidal amplitude for different boundary conditions. Zhang and Zhou [24] used a physical neutral surface to decouple the stretching–bending deformations in FGM plates and derived equations in terms of the deflection and the stress function similar to those of a homogeneous plate. For infinitesimal deformations, analytical solutions of bending of a clamped circular FGM plate under uniformly distributed load, and of buckling and free vibration of a rectangular FGM plate with simply supported edges were presented. Recently, Batra and Xiao [25] have pointed out that there is no stress tensor that is work conjugate of the von Kármán strain tensor. Thus, one should neither use the principle of minimum potential energy nor use the Hamilton principle to derive governing equations when considering the von Kármán nonlinear strains.

Different from the conventional analyses to find specific solutions for static and dynamic responses of FGM plates by using either analytical or numerical approaches, for static bending of simply supported polygonal FGM plates, Cheng and Batra [26] and Cheng and Kitipornchai [27] presented explicit relations between displacements based on the FSDT and the deflection of a homogeneous Kirchhoff plate. It can be reduced to a proportional relation between deflections of the FGM and the homogeneous Kirchhoff plates by neglecting the shear deformation. Abrate [28,29] investigated the relation between static bending, buckling and free vibration of FGM plates and corresponding homogeneous plates by examining extensive results available in the literature. He showed that the natural frequencies, the in-plane buckling loads, and the deflections of an FGM plate were proportional to those of the corresponding homogeneous plate. Even though these numerical results were obtained using the classical, the FSDT, and the TSDT, he found that the proportionality is generally applicable, the scaling factors depend on the through-the-thickness variation of the elastic modulus, and the extension-bending coupling in governing equations of thin FGM plates based on the CPT can be eliminated by using a new reference surface that is different from the midplane of the plate. However, theoretical investigations have revealed that the proportionality relation between responses of the FGM plates and those of their homogeneous counterparts is not valid when transverse shear deformations are considered. By examining the analytical bending solution of a circular FGM plate given by Reddy et al. [30] based on the FSDT and that presented by Ma and Wang [31] based on Reddy's TSDT, it can be found that there is no proportional relation between the solutions of the FGM plates and those of the corresponding homogeneous ones. However, Cheng and Batra [32] have shown that the critical buckling load and the vibration frequency for the polygonal FGM plates under in-plane hydrostatic pressure and resting on a Winkler–Pasternak elastic foundation can be expressed in terms of the eigenvalue of the clamped membrane having the shape of the plate. They showed that this correspondence is valid when the polygonal FGM plate's deformations are governed by either the TSDT, or the FSDT or the CPT, and whether or not Poisson's ratio varies through the plate thickness. Furthermore, the plate material could be transversely isotropic with the thickness direction coincident with the axis of transverse isotropy. It seems that all conditions on stiffnesses of inhomogeneous plates that must be satisfied for such correspondence relations to hold may not have been delineated.

In this paper, we use the CPT to analytically derive correspondence relations between solutions for bending, buckling and free vibrations of the FGM plates, and those of the corresponding reference homogeneous plate (RHP) with the same geometry, loading, and boundary conditions as the FGM plate. This correspondence is valid for arbitrary shaped plates and boundary conditions provided that the governing equations and the boundary conditions are linear. By using the origin of the rectangular Cartesian coordinate system in the plate midsurface, we derive a condition on the plate stiffness for the existence of the physical neutral surface. The significance of the work is that the correspondence relation enables one to solve problems for the FGM plates from the solution of the corresponding problem for the RHP. The correspondence relation is also valid for laminated plates provided that they can be modeled as isotropic, and the governing equations and the boundary conditions are linear.

2 Problem Solutions

2.1 Governing Equations. Consider a thin flat isotropic FGM plate of thickness h, with piecewise continuous variation of material properties in the thickness direction. Without loss of generality, we select a rectangular Cartesian coordinate system (x, y, z) with the x- and the y-axes located in the geometric midplane of the plate, and the z-axis along the normal to the plate midsurface. We assume that material properties of the FGM plate, such as Young's modulus, E, Poisson's ratio, ν, and the mass density, ρ, are piecewise continuous functions over the thickness, and can be described by

$$P(z) = P_b \psi_P(z) \tag{1}$$

where P_t and P_b denote, respectively, the material property values at points on the top and the bottom surfaces of the plate, and $\psi_P(z)$ is a piecewise continuous function of z that satisfies $\psi_P(-h/2) = 1$ and $\psi_P(h/2) = P_t/P_b$ at the bottom and the top surfaces, respectively.

In the CPT the displacement field is assumed to be given by

$$u(x,y,z,t) = u_0(x,y,t) - z\frac{\partial w_0}{\partial x} \tag{2a}$$

$$v(x,y,z,t) = v_0(x,y,t) - z\frac{\partial w_0}{\partial y} \tag{2b}$$

$$w(x,y,z,t) = w_0(x,y,t) \tag{2c}$$

where t is time, and u, v, and w are the x, y, and z components of the displacement field, respectively; u_0, v_0, and w_0 are the displacement components defined at the geometric mid-surface.

By using the linear strain–displacement relations and Hooke's law, we obtain the following expressions for the resultant forces and the bending moments:

$$\begin{pmatrix} N_x \\ N_y \\ N_{xy} \end{pmatrix} = \begin{bmatrix} A_{11} & A_{12} & 0 \\ A_{12} & A_{11} & 0 \\ 0 & 0 & A_{33} \end{bmatrix} \begin{pmatrix} \varepsilon_x^0 \\ \varepsilon_y^0 \\ \gamma_{xy}^0 \end{pmatrix} + \begin{bmatrix} B_{11} & B_{12} & 0 \\ B_{12} & B_{11} & 0 \\ 0 & 0 & B_{33} \end{bmatrix} \begin{pmatrix} \kappa_x \\ \kappa_y \\ \kappa_{xy} \end{pmatrix} \tag{3a}$$

$$\begin{pmatrix} M_x \\ M_y \\ M_{xy} \end{pmatrix} = \begin{bmatrix} B_{11} & B_{12} & 0 \\ B_{12} & B_{11} & 0 \\ 0 & 0 & B_{33} \end{bmatrix} \begin{pmatrix} \varepsilon_x^0 \\ \varepsilon_y^0 \\ \gamma_{xy}^0 \end{pmatrix} + \begin{bmatrix} D_{11} & D_{12} & 0 \\ D_{12} & D_{11} & 0 \\ 0 & 0 & D_{33} \end{bmatrix} \begin{pmatrix} \kappa_x \\ \kappa_y \\ \kappa_{xy} \end{pmatrix} \tag{3b}$$

In Eq. (3) the in-plane strains and curvatures are given by

$$\left(\varepsilon_x^0, \varepsilon_y^0, \gamma_{xy}^0\right) = \left(\frac{\partial u_0}{\partial x}, \frac{\partial v_0}{\partial y}, \frac{\partial v_0}{\partial x} + \frac{\partial u_0}{\partial y}\right) \tag{4a}$$

$$(\kappa_x, \kappa_y, \kappa_{xy}) = \left(-\frac{\partial^2 w_0}{\partial x^2}, -\frac{\partial^2 w_0}{\partial y^2}, -2\frac{\partial^2 w_0}{\partial x \partial y}\right) \tag{4b}$$

and the resultant forces and the bending moments are defined as

$$(N_x, N_y, N_{xy}) = \int_{-h/2}^{h/2} (\sigma_x, \sigma_y, \tau_{xy}) \mathrm{d}z \tag{5a}$$

$$(M_x, M_y, M_{xy}) = \int_{-h/2}^{h/2} (\sigma_x, \sigma_y, \tau_{xy}) z \mathrm{d}z \tag{5b}$$

The stiffness coefficients in Eq. (3) have the following expressions:

$$(A_{11}, A_{12}, A_{33}) = \int_{-h/2}^{h/2} \frac{E}{1-\nu^2}\left(1, \nu, \frac{1-\nu}{2}\right) \mathrm{d}z \tag{5c}$$

$$(B_{11}, B_{12}, B_{33}) = \int_{-h/2}^{h/2} \frac{zE}{1-\nu^2}\left(1, \nu, \frac{1-\nu}{2}\right) \mathrm{d}z \tag{5d}$$

$$(D_{11}, D_{12}, D_{33}) = \int_{-h/2}^{h/2} \frac{z^2E}{1-\nu^2}\left(1, \nu, \frac{1-\nu}{2}\right) \mathrm{d}z \tag{5e}$$

One can show that these stiffness coefficients satisfy

$$A_{12} + 2A_{33} = A_{11}, \quad B_{12} + 2B_{33} = B_{11}, \quad D_{12} + 2D_{33} = D_{11} \tag{6}$$

Ignoring in-plane inertia forces, equations of motion of the plate are

$$\frac{\partial N_x}{\partial x} + \frac{\partial N_{xy}}{\partial y} = 0, \quad \frac{\partial N_{xy}}{\partial x} + \frac{\partial N_y}{\partial y} = 0 \tag{7a,b}$$

$$\frac{\partial^2 M_x}{\partial x^2} + 2\frac{\partial^2 M_{xy}}{\partial x \partial y} + \frac{\partial^2 M_y}{\partial y^2} + N_{x0}\frac{\partial^2 w_0}{\partial x^2} + 2N_{xy0}\frac{\partial^2 w_0}{\partial x \partial y} + N_{y0}\frac{\partial^2 w_0}{\partial y^2} + q = \bar{\rho} h \frac{\partial^2 w_0}{\partial t^2} \tag{8}$$

where $q = q(x, y)$ is a transverse distributed load; N_{x0}, N_{y0}, and N_{xy0} are membrane forces in the undeformed configuration due to the applied in-plane forces at the plate edges, and $\bar{\rho}$ is the mean areal mass density defined by

$$\bar{\rho} = \frac{1}{h}\int_{-h/2}^{h/2} \rho \mathrm{d}z \tag{9}$$

Substituting from Eqs. (3) and (4) into Eqs. (7) and (8), and using relations given in Eq. (6), we get the following equations of motion in terms of displacement components:

$$A_{11}\frac{\partial^2 u_0}{\partial x^2} + A_{33}\frac{\partial^2 u_0}{\partial y^2} + (A_{12} + A_{33})\frac{\partial^2 v_0}{\partial x \partial y} = B_{11}\frac{\partial}{\partial x}\nabla^2 w_0 \tag{10}$$

$$A_{11}\frac{\partial^2 v_0}{\partial y^2} + A_{33}\frac{\partial^2 v_0}{\partial x^2} + (A_{12} + A_{33})\frac{\partial^2 u_0}{\partial x \partial y} = B_{11}\frac{\partial}{\partial y}\nabla^2 w_0 \tag{11}$$

$$D_{11}\nabla^4 w_0 + \bar{\rho} h \frac{\partial^2 w_0}{\partial t^2} = q + N_{x0}\frac{\partial^2 w_0}{\partial x^2} + 2N_{xy0}\frac{\partial^2 w_0}{\partial x \partial y} + N_{y0}\frac{\partial^2 w_0}{\partial y^2} + B_{11}\nabla^2\left(\frac{\partial u_0}{\partial x} + \frac{\partial v_0}{\partial y}\right) \tag{12}$$

where $\nabla^2 = (\partial^2/\partial x^2 + \partial^2/\partial y^2)$ is the Laplace operator and $\nabla^4 = \nabla^2\nabla^2$.

2.2 Correspondence Relations. Differentiating both sides of Eqs. (10) and (11), respectively, with respect to x and y, adding respective sides, and using Eq. (6), we obtain

$$\nabla^2\left(\frac{\partial u_0}{\partial x} + \frac{\partial v_0}{\partial y}\right) = \frac{B_{11}}{A_{11}}\nabla^4 w_0 \tag{13}$$

Substitution from Eq. (13) into Eq. (12), gives the following uncoupled equation of motion in terms of the transverse deflection w_0:

$$\nabla^4 w_0 - \frac{1}{D^*}\left(N_{x0}\frac{\partial^2 w_0}{\partial x^2} + 2N_{xy0}\frac{\partial^2 w_0}{\partial x \partial y} + N_{y0}\frac{\partial^2 w_0}{\partial y^2}\right) + \frac{\bar{\rho} h}{D^*}\frac{\partial^2 w_0}{\partial t^2} = \frac{q}{D^*} \tag{14}$$

where

$$D^* = D_{11} - B_{11}^2/A_{11} \tag{15}$$

is the equivalent flexural stiffness coefficient of the plate. Abrate [29] derived Eq. (14) by selecting a reference surface different from the geometric midsurface to eliminate the extension–bending coupling. Here, we select an RHP with material properties of the bottom surface ($E = E_b$, $\nu = \nu_b$, $\rho = \rho_b$) and define dimensionless stiffness and inertia coefficients as

$$\phi_0 = \frac{A_{11}}{C_b}, \quad \phi_1 = \frac{B_{11}}{hC_b}, \quad \phi_2 = \frac{D_{11}}{D_b}, \quad \bar{\phi}_0 = \frac{\bar{\rho}}{\rho_b} \tag{16}$$

where $C_b = E_b h/(1 - \nu_b{}^2)$ and $D_b = C_b h^2/12$ are the tension and the bending stiffnesses of the RHP, respectively. Substituting from Eq. (16) into Eq. (15), the equivalent bending stiffness coefficient D^* can be written as

$$D^* = \frac{D_b}{c}, \quad c = \frac{1}{\phi_2 - 12\phi_1{}^2/\phi_0} \tag{17}$$

where c is a dimensionless parameter which integrates effects of the transverse inhomogeneity of the plate material. We note that $c = 1$ for the RHP.

From the three coupled equilibrium Eqs. (10)–(12) in terms of the three displacement components at a point on the plate's geometric midsurface, we have derived the uncoupled governing Eq. (14) for the transverse deflection of the plate midsurface. This equation with D^* replaced by D_b is the transverse deflection equation for the RHP. By assuming that Poisson's ratio is a constant and using the concept of the physical neutral surface to eliminate the bending–tension coupling in the deformation, Zhang and Zhou [24] also derived Eq. (14).

2.3 Physical Neutral Surface. In the absence of constraints at the boundaries to prevent in-plane movements, the membrane forces will vanish. Thus,

$$N_x = A_{11}\frac{\partial u_0}{\partial x} + A_{12}\frac{\partial v_0}{\partial y} - B_{11}\frac{\partial^2 w_0}{\partial x^2} - B_{12}\frac{\partial^2 w_0}{\partial y^2} = 0 \tag{18}$$

$$N_y = A_{12}\frac{\partial u_0}{\partial x} + A_{11}\frac{\partial v_0}{\partial y} - B_{12}\frac{\partial^2 w_0}{\partial x^2} + B_{11}\frac{\partial^2 w_0}{\partial y^2} = 0 \quad (19)$$

$$N_{xy} = A_{33}\left(\frac{\partial u_0}{\partial y} + \frac{\partial v_0}{\partial x}\right) - 2B_{33}\frac{\partial^2 w_0}{\partial x \partial y} = 0 \quad (20)$$

If the stiffnesses also satisfy the relation, $A_{11}B_{12} = A_{12}B_{11}$, then from Eqs. (18)–(20) one can deduce that

$$\frac{\partial u_0}{\partial x} = z_0\frac{\partial^2 w_0}{\partial x^2}, \quad \frac{\partial v_0}{\partial y} = z_0\frac{\partial^2 w_0}{\partial y^2}, \quad \frac{\partial u_0}{\partial y} + \frac{\partial v_0}{\partial x} = 2z_0\frac{\partial^2 w_0}{\partial x \partial y} \quad (21a,b,c)$$

where the constant z_0 is given by

$$z_0 = \frac{B_{11} - B_{12}}{A_{11} - A_{12}} = \frac{B_{33}}{A_{33}} = \frac{B_{11}}{A_{11}} = \frac{h\phi_1}{\phi_0} \quad (22)$$

Recalling Eqs. (3) and (5), the relation $A_{11}B_{12} = A_{12}B_{11}$ implies that the Poisson effect for stretching and stretching–bending coupling deformations is the same.

By integrating Eqs. (21*a*) and (21*b*), it is easy to get a general solution for the in-plane displacements

$$u_0 = z_0\frac{\partial w_0}{\partial x} + f(y,t), \quad v_0 = z_0\frac{\partial w_0}{\partial y} + g(x,t) \quad (23)$$

where $f(y,t)$ and $g(x,t)$ are arbitrary functions. Substituting Eq. (23) into Eq. (21*c*) yields

$$\frac{\partial f(y,t)}{\partial y} = -\frac{\partial g(x,t)}{\partial x} = \alpha_1(t) \quad (24)$$

which gives

$$f(y,t) = \alpha_1 y + \alpha_2, \quad g(x,t) = -\alpha_1 x + \alpha_3 \quad (25)$$

where α_i $(i = 1,2,3)$ are at most functions of time, t. One can easily show that $f(y,t)$ and $g(x,t)$ are the rigid body displacements which vanish in a plate if boundary conditions at its edges rule out rigid body motion. Henceforth, we assume that this is the case. Substituting from Eq. (23) (with $f = g = 0$) into Eqs. (2*a*) and (2*b*) we get

$$u(x,y,z,t) = (z_0 - z)\frac{\partial w_0}{\partial x}, \quad v(x,y,z,t) = (z_0 - z)\frac{\partial w_0}{\partial y} \quad (26a,b)$$

Thus the physical neutral surface of the FGM plate [14,24] is given by $z = z_0$. By using Eq. (26), or the definition of the physical neutral surface, one can also uncouple governing Eq. (14) instead of eliminating the in-plane displacements from Eqs. (11)–(13). It should be noted that Eqs. (18)–(20) together with the constraint $A_{11}B_{12} = A_{12}B_{11}$ must hold for the physical neutral surface to exist. Therefore, if either the boundary conditions at the plate edges constrain the in-plane displacements or geometric nonlinearities are considered or the material inhomogeneity is such that $A_{11}B_{12} \neq A_{12}B_{11}$, then Eq. (26) cannot be derived.

Substituting from Eq. (23) into Eq. (3) and assuming that the Poisson ratio is constant through the plate thickness, we can express bending moments in terms of curvatures as

$$M_x = -D^*\left(\frac{\partial^2 w_0}{\partial x^2} + \nu\frac{\partial^2 w_0}{\partial y^2}\right) \quad (27a)$$

$$M_y = -D^*\left(\frac{\partial^2 w_0}{\partial y^2} + \nu\frac{\partial^2 w_0}{\partial x^2}\right) \quad (27b)$$

$$M_{xy} = -2(1-\nu)D^*\frac{\partial^2 w_0}{\partial x \partial y} \quad (27c)$$

Furthermore, substitution from Eq. (27) into equilibrium equations

$$\frac{\partial M_x}{\partial x} + \frac{\partial M_{xy}}{\partial y} = Q_x, \quad \frac{\partial M_{xy}}{\partial x} + \frac{\partial M_y}{\partial y} = Q_y \quad (28a,b)$$

yields

$$Q_x = -D^*\frac{\partial}{\partial x}\nabla^2 w_0, \quad Q_y = -D^*\frac{\partial}{\partial y}\nabla^2 w_0 \quad (28c,d)$$

where Q_x and Q_y are the resultant shear forces per unit length along the x- and the y-axes, respectively. In summary, we have derived Eqs. (14) and (26)–(28) for the FGM plate which are the same as those for the RHP when D^* is replaced by D_b. Of course, the boundary conditions for the two plates must also have similar correspondence.

3 Correspondence Relations Between Solutions for the FGM Plate and the RHP

3.1 Static Bending. For static bending of a plate, we have $w_0(x,y,t) = \bar{w}(x,y)$ and Eq. (14) reduces to

$$\frac{D_b}{c}\nabla^4\bar{w} = q \quad (29)$$

For $c = 1$, Eq. (29) is the governing equation of the RHP subjected to the same loading as the FGM plate. If $\bar{w}_h(x,y)$ is the particular solution of Eq. (29) for $c = 1$ and the specified boundary conditions, then

$$\bar{w}(x,y) = c\,\bar{w}_h(x,y) + \Phi(x,y) \quad (30)$$

where $\bar{w}(x,y)$ is the solution for the FGM plate and the function $\Phi(x,y)$ satisfies the differential equation $\nabla^4\Phi(x,y) = 0$ and the associated *homogeneous boundary conditions*. The theory of linear differential equations with the homogeneous boundary conditions gives $\Phi(x,y) \equiv 0$. Thus, we have $\bar{w}(x,y) = c\,\bar{w}_h(x,y)$, where the scaling factor c is given by Eq. (17). We note that solutions of Chi and Chung [10] for the deflection of the simply supported rectangular FGM plate satisfy Eq. (30).

3.2 Static Buckling. For the static buckling of an FGM plate, Eq. (15) becomes

$$\nabla^4\bar{w} - \frac{c}{D_b}\left(N_{x0}\frac{\partial^2\bar{w}}{\partial x^2} + 2N_{xy0}\frac{\partial^2\bar{w}}{\partial x \partial y} + N_{y0}\frac{\partial^2\bar{w}}{\partial y^2}\right) = 0 \quad (31)$$

where the initial in-plane membrane forces can be independently determined by solving prebuckling deformations of the plate. We assume that the in-plane loads are such that

$$N_{x0} = \lambda_1 P, \quad N_{y0} = \lambda_2 P, \quad N_{xy0} = \lambda_3 P \quad (32)$$

where P is a load parameter and λ_i $(i = 1,2,3)$ are scaling constants. Substitution from Eq. (32) into Eq. (31) yields

$$\nabla^4\bar{w} + \frac{cP}{D_b}\left(\lambda_1\frac{\partial^2\bar{w}}{\partial x^2} + 2\lambda_3\frac{\partial^2\bar{w}}{\partial x \partial y} + \lambda_2\frac{\partial^2\bar{w}}{\partial y^2}\right) = 0 \quad (33)$$

For $c = 1$, Eq. (33) reduces to

$$\nabla^4\bar{w}_h - \frac{P_h}{D_b}\left(\lambda_1\frac{\partial^2\bar{w}_h}{\partial x^2} + 2\lambda_3\frac{\partial^2\bar{w}_h}{\partial x \partial y} + \lambda_2\frac{\partial^2\bar{w}_h}{\partial y^2}\right) = 0 \quad (34)$$

that governs the buckling of the RHP. If P_{hcr} is a critical buckling load for the RHP, or the minimum eigenvalue of differential

Eq. (34) with the prescribed boundary conditions and $\bar{w}_{\mathrm{hcr}}$ is the corresponding buckling mode shape, then the similarity between Eqs. (33) and (34) gives

$$\bar{w}_{\mathrm{cr}} = c\bar{w}_{\mathrm{hcr}}, \quad P_{\mathrm{cr}} = P_{\mathrm{hcr}}/c \tag{35}$$

where P_{cr} and $\bar{w}_{\mathrm{cr}}$ are the critical buckling load and the related mode shape of the FGM plate.

3.3 Free Vibration. Setting $q = N_{x0} = N_{y0} = N_{xy0} = 0$ in Eq. (15) yields the equation of motion for free vibrations of the FGM plate. Furthermore, assuming a harmonic response of the system given by

$$w_0(x, y, t) = \bar{w}(x, y)\cos\omega t \tag{36}$$

and substituting it into Eq. (15) yields the following equation governing the mode shape $\bar{w}$:

$$\nabla^4\bar{w} - \omega^2\frac{c_\rho h\rho_b}{D_b}\bar{w} = 0, \quad c_\rho = c\bar{\phi}_0 \tag{37}$$

Here, ω is a natural frequency of the FGM plate. For $c_\rho = 1$, Eq. (37) reduces to the following governing equation for the RHP:

$$\nabla^4\bar{w}_h - {\omega_h}^2\frac{\rho_b h}{D_b}\bar{w}_h = 0 \tag{38}$$

Here ω_h is a natural frequency of the RHP. The similarity between Eqs. (37) and (38) yields

$$\bar{w} = c\bar{w}_h, \quad \omega = \omega_h/\sqrt{c_\rho} \tag{39}$$

3.4 Discussion of Boundary Conditions. When homogeneous essential boundary conditions (i.e., either w_0 or $(\partial w_0/\partial x)$ or $(\partial w_0/\partial y)$ or their linear combination) are prescribed at an edge then both $\bar{w}_h(x, y)$ and $\bar{w}(x, y)$ will satisfy them.

Natural boundary conditions involve specifying either the bending moments or the resultant shear forces. Substitution of $w_0 = \bar{w} = c\bar{w}_h$ into Eqs. (27) and (28) yields

$$M_x = M_{hx}, \quad M_y = M_{hy}, \quad M_{xy} = M_{hxy} \tag{40a,b,c}$$

$$Q_x = Q_{hx}, \quad Q_y = Q_{hy} \tag{41a,b}$$

where quantities with the superscript, h, are those for the RHP. Thus, the shear forces and bending moments for the FGMP are the same as those of the RHP. So, if solution $\bar{w}_h$ satisfies the natural boundary conditions

$$M_{hn} = M_n^*, \quad R_{hn} = Q_{hn} + \frac{\partial M_{hsn}}{\partial s} = R_n^* \tag{42}$$

at boundary S_σ, then the deflection, $\bar{w}$, satisfies boundary conditions for the FGMP on S_σ. Here M_n^* and R_n^* are the prescribed moment and force at S_σ, n and s represent, respectively, the unit normal and the unit tangent at a boundary point.

4 Example Problems

In this section, numerical results for the FGM plate (FGMP) are presented to show the validity of the proposed correspondence between quantities for the FGMP and those for the RHP. It is assumed that the FGMP is composed of a ceramic (alumina) and a metal (aluminum) with the function $\psi_P(z)$ in Eq. (1) given by

$$\psi_P = 1 + \left(\frac{P_t}{P_b} - 1\right)\left(\frac{1}{2} + \frac{z}{h}\right)^n \tag{43}$$

where n is the material gradient parameter having values in the interval $[0, \infty)$. The Poisson ratio is assumed to be constant, $\nu \equiv 0.3$. Values assigned to Young's modulus and the mass density are [9,14]

ceramic (alumina): $E_c = E_t = 380\,\mathrm{GPa}$, $\rho_c = \rho_t = 3800\,\mathrm{kg/m^3}$
metal (aluminum): $E_m = E_b = 70\,\mathrm{GPa}$, $\rho_m = \rho_b = 2707\,\mathrm{kg/m^3}$

Substituting for functions $\psi_E(z)$ and $\psi_\rho(z)$ from Eq. (43) into Eqs. (5) and (16) yields

$$\begin{aligned} \phi_0 &= 1 + \frac{r_E - 1}{n+1}, \quad \phi_1 = \frac{n(r_E - 1)}{2(n+1)(n+2)}, \\ \phi_2 &= 1 + \frac{3(r_E - 1)(n^2 + n + 2)}{(n+1)(n+2)(n+3)}, \quad \bar{\phi}_0 = 1 + \frac{r_\rho - 1}{n+1} \end{aligned} \tag{44}$$

where $r_E = E_t/E_b$, $r_\rho = \rho_t/\rho_b$. Substitution from Eq. (44) into Eqs. (17) and (37) gives the transition parameters, c and c_ρ, as

Table 1 Values of the dimensionless coefficients $\phi_i (i=0,1,2)$, $\bar{\phi}_0$, c, and c_ρ for specified values of the material gradient index, n

n	0	0.5	1	3	5	7	10	100	∞
ϕ_0	5.4286	3.9524	3.2143	2.1071	1.7381	1.5536	1.4026	1.0438	1
ϕ_1	0	0.2952	0.3691	0.3321	0.2636	0.2153	0.1678	0.0215	0
ϕ_2	5.4286	3.7837	3.2143	2.5500	2.2653	2.0702	1.8671	1.1265	1
$\bar{\phi}_0$	1.4038	1.2692	1.2019	1.1009	1.0673	1.0505	1.0367	1.0040	1
c	0.1842	0.2842	0.3696	0.5204	0.5601	0.5840	0.6149	0.8919	1
c_ρ	0.5085	0.6006	0.6665	0.7569	0.7731	0.7833	0.7984	0.9463	1

Table 2 Dimensionless deflections at the centroid of a simply supported square FGM plate under either a transverse uniform distributed load, q_0, or a concentrated force, F

	n								
	0	0.2	0.5	1	2	3	10	100	∞
$\frac{\bar{w}_c D_b}{q_0 a^4} \times 10^3$	0.7483[a]	0.9127	1.1543	1.5012	1.9238	2.1137	2.4976	3.6230	4.0620
	0.7483[b]	0.9127	1.1544	1.5013	1.9239	2.1138	2.4977	3.6232	4.0622
$\frac{\bar{w}_c D_b}{F a^2} \times 10^3$	2.1371[a]	2.6066	3.2968	4.2876	5.4947	6.0370	7.1333	10.348	11.602
	2.1371[b]	2.6066	3.2968	4.2876	5.4947	6.0370	7.1333	10.348	11.602

[a]By Eq. (30).
[b]By FEM; $\bar{w}_c$ is deflection at the plate centroid.

Table 3 Comparison of dimensionless centroidal deflection, $W_0 = 64D_b/(q_0R^4\bar{w}_0)$, of circular FGM plates obtained by Eq. (30) with those in the literature (E_t/E_b=0.396, $\nu_b=\nu_t$=0.288)

	Clamped				Roller-supported	
n	Ref. [30]	Ref. [31]	Ref. [24]	Eq. (30)	Ref. [30]	Eq. (30)
0	5.525	5.525	5.525	5.5253	10.386	10.368
2	1.388	1.389	1.388	1.3882	5.700	5.6996
4	1.269	1.269	1.269	1.2690	5.210	5.2099
6	1.208	1.208	1.208	1.2076	4.958	4.9581
8	1.169	1.169	1.169	1.1692	4.800	4.8002
10	1.143	1.143	1.143	1.1427	4.692	4.6916
20	1.080	1.080	1.080	1.0800	4.434	4.4340
30	1.056	1.056	1.056	1.0555	4.334	4.3336
40	1.043	1.043	1.048	1.0425	4.280	4.2801
50	1.034	1.034	1.034	1.0344	4.247	4.2450
100	1.018	1.018	1.018	1.0177	4.178	4.1781
10^5	1.000	—	—	1.0000	4.106	4.1062

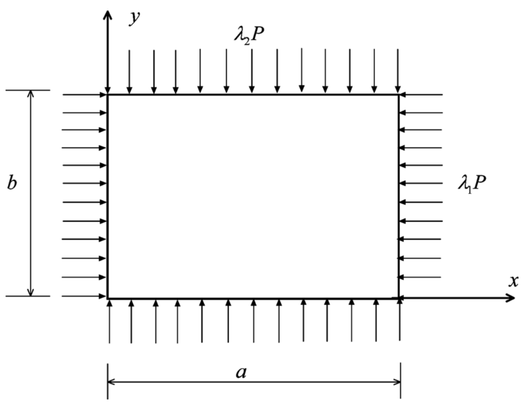

Fig. 1 Rectangular plates subjected to in-plane uniformly distributed loads

functions of the power index, n. Values of coefficients $\phi_i (i = 0, 1, 2)$ and $\bar{\phi}_0$ for some values of n are listed in Table 1.

In Table 2, dimensionless centroidal deflections for different values of n of a simply supported square FGMP subjected to either uniformly distributed load, q_0, or concentrated force, F, at the plate center computed by two methods are compared. In Table 3, dimensionless centroidal deflections of a thin circular FGM plate under axisymmetric bending subjected to a uniformly distributed load and computed by using the correspondence relation are compared with those available in the literature [24,30,31] for the circular FGMP with R being the radius of the circular plate. Excellent agreement between the present results and those in the literature shows the validity of Eq. (30) for giving an accurate bending solution of an FGMP in terms of that of the RHP.

Another example problem studied is the buckling of a rectangular FGMP with length a, width b, and thickness h subjected to in-plane compressive forces $\lambda_1 P$ and $\lambda_2 P$ in the x- and the y-directions, respectively, as shown in Fig. 1. In Table 4, we have listed the critical buckling load, P_{cr}, of the FGMP with SSSS (all edges simply supported) and SCSC (two opposite edges simply supported and the other two edges clamped) boundary conditions obtained from Eq. (35), the FEM and the Levy analytical solution [9], respectively. It is clear that results from Eq. (35) agree well with those given by the two other approaches.

Finally, we study free vibration of a square FGMP. In order to show the validity of the correspondence relation for the frequencies, the first five dimensionless frequencies of the square FGMP

Table 4 Critical buckling load P_{cr} (MN/m) for an FGMP with different boundary conditions for specified values of the gradient index n and aspect ratio a/b ($h/b = 0.01$)

			$\lambda_1 = 1,\ \lambda_2 = 0,\ \lambda_3 = 0$			$\lambda_1 = 1,\ \lambda_2 = 1,\ \lambda_3 = 0$		
BCs	N	a/b	FEM	Equation (35)	[9]	FEM	Equation (35)	[9]
SSSS	0	0.5	2.1444	2.1466	2.1466	1.7155	1.7173	1.7172
		1	1.3727	1.3738	1.3738	0.6863	0.6869	0.6869
	1	0.5	1.0689	1.0698	1.0699	0.8551	0.8559	0.8559
		1	0.6842	0.6847	0.6848	0.3421	0.3423	0.3424
	2	0.5	0.8341	0.8349	0.8349	0.6672	0.6679	0.6679
		1	0.5339	0.5343	0.5343	0.2669	0.2672	0.2672
SCSC	0	0.5	2.6381	2.6417	2.6416	2.0318	2.0348	2.0347
		1	2.6359	2.6417	2.6416	1.3137	1.3154	1.3154
	1	0.5	1.3149	1.3166	1.3167	1.0127	1.0141	1.0142
		1	1.3138	1.3166	1.3167	0.6548	0.6556	0.6556
	2	0.5	1.0261	1.0275	1.0274	0.7903	0.7914	0.7914
		1	1.0252	1.0275	1.0274	0.5109	0.5116	0.5116
SFSF	0	0.5	1.3376	1.3370	1.3369	1.3097	1.3086	1.3085
		1	0.3271	0.3271	0.3271	0.3203	0.3202	0.3202
	1	0.5	0.6667	0.6663	0.6664	0.6528	0.6522	0.7225[a]
		1	0.1631	0.1630	0.1630	0.1596	0.1596	0.1712
	2	0.5	0.5202	0.5200	0.5200	0.5094	0.5090	0.5089
		1	0.1272	0.12721	0.1272	0.1246	0.1245	0.1245

[a]Higher buckling mode.

Table 5 The first five dimensionless frequencies ($\Omega=\omega(a^2/h)\sqrt{\rho_b/E_b}$) of a thin square FGMP with SSSS and CSCS edges for specified values of the gradient index n

		SSSS				CSCS			
Modes	Source	$n=0.0$	$n=0.5$	$n=1.0$	$n=2.0$	$n=0.0$	$n=0.5$	$n=1.0$	$n=2.0$
1	FEM	11.746	9.9456	8.9618	8.1478	17.226	14.587	13.144	11.950
	[14]	11.746	9.9456	8.9618	8.1478	17.227	14.587	13.144	11.950
	Equation (39)	11.747	9.9464	8.9626	8.1486	17.226	14.587	13.142	11.950
2	FEM	29.361	24.862	22.403	20.368	32.568	27.577	24.849	22.592
	[14]	29.361	24.861	22.402	20.367	32.571	27.578	24.851	22.593
	Equation (39)	29.367	24.866	22.407	20.372	32.575	27.584	24.855	22.598
3	FEM	29.361	24.862	22.403	20.368	41.248	34.927	31.472	28.614
	[14]	29.361	24.861	22.402	20.367	41.248	34.926	31.471	28.612
	Equation (39)	29.367	24.866	22.407	20.372	41.256	34.933	31.478	28.619
4	FEM	46.966	39.768	35.835	32.580	56.256	47.635	42.923	39.025
	[14]	46.971	39.773	35.839	32.584	56.269	47.645	42.932	39.031
	Equation (39)	46.986	39.786	35.850	32.594	56.287	47.661	42.947	39.046
5	FEM	58.722	49.723	44.804	40.735	60.810	51.491	46.398	42.184
	[14]	58.712	49.714	44.798	40.729	60.807	51.488	46.394	42.178
	Equation (39)	58.733	49.732	44.813	40.743	60.798	51.480	46.388	42.175

with the SSSS and SCSC boundary conditions, obtained from Eq. (39), the FEM and that computed using the nonuniform rational B-spline basis functions [14] are presented in Table 5 for some values of n. It is obvious that results from Eq. (39) match well with those deduced from the other two approaches.

5 Remarks

The correspondence relations (30), (35), and (39) enable one to determine global quantities for an FGM plate from those of the corresponding RHP. However, local stresses in an FGM plate are not determined from those of the RHP. Since more than one through-the-thickness distributions of material properties can give us the same values of the parameter c defined by Eq. (17), therefore different FGM plates can have the same global response even though through-the-thickness stress distributions and the maximum principal stresses in them are quite different. Thus values of the local quantities will need to be determined from knowledge of the precise spatial variations of material parameters.

6 Conclusions

We have used the CPT to analytically deduce the exact proportional relations between solutions for bending, buckling and free vibration of the FGM plates with an arbitrary through-the-thickness variation in the material properties and those of the RHP of the same geometry, loadings and boundary conditions as the FGM plate. Thus, solutions for isotropic FGM and other inhomogeneous (e.g., laminated) isotropic plates can be derived from those of the corresponding homogeneous plates available in the literature. However, a physical neutral surface for the FGM plates exists provided that bending and stretching stiffnesses satisfy a condition, the Poisson ratio is constant, and there are no in-plane forces induced by the boundary conditions.

Acknowledgment

SRL's work was supported by the National Natural Science Foundation of China Grant No. 11272278. RCB's work was partially supported by the U.S. Office of Naval Research Grant No. N00014-11-1-0594 to Virginia Polytechnic Institute and State University with Dr. Rajapakse as the Program Manager. The authors gratefully acknowledge the financial support received for the work.

References

[1] Qian, L. F., and Batra, R. C., 2005, "Design of Bidirectional Functionally Graded Plate for Optimal Natural Frequencies," J. Sound Vib., **280**(1–2), pp. 415–424.

[2] Liu, D. Y., Wang, C. Y., and Chen, W. Q., 2010, "Free Vibration of FGM Plates With In-Plane Material Inhomogeneity," Compos. Struct., **92**(5), pp. 1047–1051.

[3] Jha, D. K., Kant, T., and Singh, R. K., 2013, "A Critical Review of Recent Research on Functionally Graded Plates," Compos. Struct., **96**, pp. 833–849.

[4] Swaminathan, K., Naveenkumar, D. T., Zenkour, A. M., and Carrera, E., 2015, "Stress, Vibration and Buckling Analyses of FGM Plates—A State-of-the-Art Review," Compos. Struct., **120**, pp. 10–31.

[5] Yang, J., and Shen, H. S., 2001, "Dynamic Response of Initially Stressed Functionally Graded Rectangular Thin Plates," Compos. Struct., **54**(4), pp. 497–508.

[6] He, X. Q., Ng, T. Y., Sivashanker, S., and Liew, K. M., 2001, "Active Control of FGM Plates With Integrated Piezoelectric Sensors and Actuators," Int. J. Solids Struct., **38**(9), pp. 1641–1655.

[7] Javaheri, R., and Eslami, M. R., 2002, "Buckling of Functionally Graded Rectangular Plates Under In-Plane Compressive Loading," ZAMM, **82**(4), pp. 277–283.

[8] Samsarn Shariata, B. A., Javaheri, R., and Eslami, M. R., 2005, "Buckling of Imperfect Functionally Graded Plates Under In-Plane Compressive Loading," Thin-Walled Struct., **43**(7), pp. 1020–1036.

[9] Mohammadi, M., Saidi, A. R., and Jomehzadeh, E., 2010, "Levy Solution for Buckling Analysis of Functionally Graded Rectangular Plates," Appl. Compos. Mater., **17**(2), pp. 81–93.

[10] Chi, S.-H., and Chung, Y.-L., 2006, "Mechanical Behavior of Functionally Graded Material Plates Under Transverse Load—Part I: Analysis," Int. J. Solids Struct., **43**(13), pp. 3657–3674.

[11] Chi, S.-H., and Chung, Y.-L., 2006, "Mechanical Behavior of Functionally Graded Material Plates Under Transverse Load—Part II: Numerical Results," Int. J. Solids Struct., **43**(13), pp. 3675–3691.

[12] Nie, G. J., and Batra, R. C., 2010, "Exact Solutions and Material Tailoring for Functionally Graded Hollow Circular Cylinders," J. Elasticity, **99**(2), pp. 179–201.

[13] Zimmerman, R. W., and Lutz, M. P., 1999, "Thermal Stresses and Thermal Expansion in a Uniformly Heated Functionally Graded Cylinder," J. Therm. Stresses, **22**(2), pp. 177–188.

[14] Yin, S.-H., Yu, T. T., and Liu, P., 2013, "Free Vibration Analyses of FGM Thin Plates by Isogeometric Analysis Based on Classical Plate Theory and Physical Neutral Surface," Adv. Mech. Eng., **2013**, p. 634584.

[15] Ebrahimi, F., and Rastgo, A., 2008, "An Analytical Study on the Free Vibration of Smart Thin FGM Plate Based on Classical Plate Theory," Thin-Walled Struct., **46**(12), pp. 1402–1408.

[16] Ebrahimi, F., and Rastgo, A., 2008, "Free Vibration Analysis of Smart Annular FGM Plates Integrated With Piezoelectric Layers," Smart Mater. Struct., **17**(1), p. 015044.

[17] Mirtalaie, S.-H., and Hajabasi, M. A., 2011, "Free Vibration Analysis of Functionally Graded Thin Annular Sector Plates Using the Differential Quadrature Method," Proc. Inst. Mech. Eng., Part C, **225**(3), pp. 568–583.

[18] Hasani Baferani, A., Saidi, A. R., and Jomehzadeh, E., 2011, "An Exact Solution for Free Vibration of Thin Functionally Graded Rectangular Plates," Proc. Inst. Mech. Eng., Part C, **225**(3), pp. 526–536.

[19] Vel, S. S., and Batra, R. C., 2004, "Three-Dimensional Exact Solution for the Vibration of Functionally Graded Rectangular Plates," J. Sound Vib., **272**(3–5), pp. 703–730.

[20] Vel, S. S., and Batra, R. C., 2003, "Three-Dimensional Analysis of Transient Thermal Stresses in Functionally Graded Plates," Int. J. Solids Struct., **40**(25), pp. 7181–7196.

[21] Vel, S. S., and Batra, R. C., 2002, "Exact Solutions for Thermoelastic Deformations of Functionally Graded Thick Rectangular Plates," AIAA J., **40**(7), pp. 1421–1433.

[22] Yang, J., and Shen, H.-S., 2003, "Non-Linear Analysis of Functionally Graded Plates Under Transverse and In-Plane Loads," Int. J. Non-Linear Mech., **38**(4), pp. 467–482.
[23] Woo, J., Meguid, S. A., and Ong, L. S., "Nonlinear Free Vibration Behavior of Functionally Graded Plates," J. Sound Vib., **289**(3), pp. 595–611.
[24] Zhang, D. G., and Zhou, Y. H., 2008, "A Theoretical Analysis of FGM Plate Based on Physical Neutral Surface," Comput. Mater. Sci., **44**(2), pp. 716–720.
[25] Batra, R. C., and Xiao, J., "Finite Deformations of Full Sine-Wave St.-Venant Beam Due to Tangential and Normal Distributed Loads Using Nonlinear TSNDT," Meccanica, **50**(2), pp. 355–365.
[26] Cheng, Z. Q., and Batra, R. C., 2000, "Deflection Relationship Between the Kirchhoff Plate Theory and Different Functionally Graded Plate Theory," Arch. Mech., **52**(1), pp. 143–158.
[27] Cheng, Z. Q., and Kitipornchai, S., 2000, "Exact Bending Solution of Inhomogeneous Plates From Homogeneous Thin-Plate Deflection," AIAA J., **38**(7), pp. 1289–1291.
[28] Abrate, S., 2006, "Free Vibration, Buckling, and Static Deflections of Functionally Graded Plates," Compos. Sci. Technol., **66**(14), pp. 2382–2394.
[29] Abrate, S., 2008, "Functionally Graded Plates Behave Like Homogenous Plates," Compos. Part B: Eng., **39**(1), pp. 151–158.
[30] Reddy, J. N., Wang, C. M., and Kitipomchai, S., 1999, "Axisymmetric Bending of Functionally Graded Circular Plates," Eur. J. Mech.-A/Solids, **18**(2), pp. 185–199.
[31] Ma, L. S., and Wang, T. J., 2003, "Nonlinear Bending and Post-Buckling of a Functionally, Graded Circular Plate Under Mechanical and Thermal Loadings," Int. J. Solids Struct., **40**(13–14), pp. 3311–3330.
[32] Cheng, Z. Q., and Batra, R. C., 2000, "Exact Correspondence Between Eigenvalues of Membranes and Functionally Graded Simply Supported Polygonal Plates," J. Sound Vib., **229**(4), pp. 879–895.